Stapp Car Crash Journal, Vol. 51 (October 2007), pp. 1-15

2007-22-0001

Parametric Study of Head Impact in the Infant

Brittany Coats and Susan S. Margulies
University of Pennsylvania, Department of Bioengineering

Songbai Ji
Dartmouth College, Thayer School of Engineering

ABSTRACT – Computer finite element model (FEM) simulations are often used as a substitute for human experimental head injury studies to enhance our understanding of injury mechanisms and develop prevention strategies. While numerous adult FEM of the head have been developed, there are relatively few pediatric FEM due to the paucity of material property data for children. Using radiological serial images of infants (<6wks old) and recent published material property data of infant skull and suture, we developed a FEM of the infant head to study skull fracture from occipital impacts. Here we determined the relative importance of brain material properties and anatomical variations in infant suture and scalp tissue on principal stress (σ_p) estimates in the skull of the model using parametric simulations of occipital impacts from 0.3m falls onto concrete. Decreasing the brain stiffness of pediatric brain tissue by a factor of two to simulate the softer adult brain properties we reported previously did not affect σ_p. Using adult brain stiffness reported by others (4 times higher than our pediatric values) increased σ_p in skull by 38%. Interestingly, the precision used to model compressibility of the brain (0.49-0.4999) significantly varied σ_p 30-77%, underscoring the influence of the brain properties in models of fracture in the highly deformable infant skullcase. Suture thickness, small anatomical variations in suture width and the exclusion of scalp did not affect σ_p of the skull; however, unusually large sutures (10 mm) in young infants significantly lowered σ_p. Validation of this model against published infant cadaver drop studies found good agreement with the prediction of fracture for falls onto hard surfaces. More biomechanical data from impacts onto softer surfaces is needed before skull fracture predictions can be made in these scenarios. In summary, the pediatric FEM response is not sensitive to small variations in anatomy or brain modulus, large deviations will significantly influence principal stress estimates and the prediction of skull fracture.

KEYWORDS – Finite Element Model, Pediatric, Skull Fracture, Head Impact

INTRODUCTION

Finite element model (FEM) simulations are often used to predict the adult human head response to impact (Al-Bsharat, et al. 1999; DiMasi, et al. 1995; Kleiven and von Holst 2002; Krabbel and Appel 1995; Ruan, et al. 1994; Willinger, et al. 1999; Zhang, et al. 2001), but there are relatively few three-dimensional (3D) FEM pertaining to the pediatric head. The earliest 3D model of an infant was developed by Lapeer and Prager (2001) who created detailed skull geometry from a commercial replica of a fetal skull to simulate skull deformation during vaginal birth. Material properties of dura (Bylski, et al. 1986) were used for the sutures and fontanel. The brain was not represented in the model. Intra-uterine pressures were applied to the external surface of the skull. Subsequently, a 3D model of the infant head was developed by Klinich et al (2002). The Klinich et al. model was designed as a parametric study to determine material properties that affect the stress and strains in the infant skull following frontal car impact while a child is restrained in a rear facing car seat. Klinich et al. utilized CT scans of a 27-week old infant to obtain accurate skull geometry for a finite element model of a 6-month old child. Klinich et al. used both human adult and porcine pediatric mechanical properties reported in the literature to model scalp, suture, CSF, dura, and brain. Parametric studies with this model demonstrated that suture material properties have minimal influence on the distribution of stresses throughout the skull when simulating an airbag being deployed against the rear of a child restraint system. The most critical material

Address correspondence to Susan S. Margulies, Department of Bioengineering, 240 Skirkanich Hall, University of Pennsylvania, Philadelphia, PA 19104-6321. Electronic mail: margulie@seas.upenn.edu

property was of the cranial bone itself. New data on the material properties of pediatric human cranial bone and suture has since been published (Coats and Margulies 2006) and report the average elastic modulus of human parietal and occipital bone from 11-12 month olds (E=531 MPa and 412 MPa, respectively) to be an order of magnitude less stiff than the pediatric porcine cranial bone used in the Klinich et al. model (E=3 GPa). Additionally, human pediatric cranial suture for 11-12 month olds was found to be 2 orders of magnitude less stiff than that of porcine cranial suture used in the Klinich et al. model (E_{human}=10.2 MPa vs $E_{porcine}$=1.95 GPa). These differences in material properties are beyond the range of those selected for the Klinich et al. parametric study (2002) and indicate that the prior model had a stiff skullcase which would overestimate the stress response.

The objective of this study was to develop a geometrically accurate finite element model of a 1.5 month old infant that incorporates the recently published human infant skull and suture material property data and predicts skull fracture following occipital impact from low height falls. Convergence and parametric studies were performed to determine an appropriate mesh density and to evaluate the relative importance of brain material stiffness and skullcase anatomical variations. The model's ability to predict fracture was validated by simulating parietal-occipital impacts from published infant cadaver drops 0.82 m onto stone tile (Weber 1984).

METHODS

Pediatric Head Model Development

Geometry. The geometry of the finite element model was obtained from a series of MRI and CT images of a 5-week-old infant male patient with a history of seizing. The images were determined by the Radiology Department at the Children's Hospital of Philadelphia to have no intracranial hemorrhages, midline shifts, skull fractures, swelling, or other cerebral abnormalities. The discrete boundary points of the outer surface of the skull in each MRI were detected using the canny edge detector, and an in-house program was then applied to construct closed boundary contours (Ji and Margulies 2007). The resulting geometry was imported into Rhinoceros (Robert McNeel & Associates, Seattle, WA) to construct a 3D representation of the outer surface of the skull (Figure 1). Several thickness measurements were made of the skull plates from the CT images and the outer surface of each skull plate was appropriately projected inward to form the inner skull surface. In regions where suture and fontanels were difficult to establish on either CT or MRI images, the geometry was based on an anatomical atlas of the infant skull (Crelin 1969).

The surface of the brain was created by projecting the inner surface of the skull inward by 1 mm to designate the subdural-subarachnoidal space (measured from MRI images). Because the finite element model was designed to predict skull fracture, the brain (cerebrum, cerebellum and brainstem) was assumed to be homogenous and isotropic, and the falx cerebri, ventricles, andtentorium were not included.

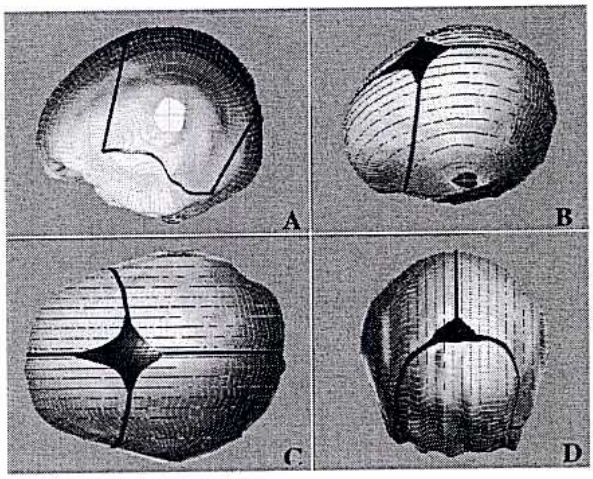

Figure 1. (A) Side, (B) 3D, (C) top, and (D) rear views of the skull and suture geometry derived from MRI and CT images of a 5 week old male infant.

Material Properties. The brain was modeled as non-linear homogeneous and isotropic hyperelastic and viscoelastic material properties using the Ogden strain energy potential as described and used previously by Prange and Margulies (2002). Pediatric brain shear modulus (μ=559 Pa, Table 1) was estimated by scaling from published human adult values (μ =257 Pa) by the ratio of shear modulus reported between newborn and adult porcine gray matter ($\mu_{newborn}$ = 2.17 μ_{adult}) also reported in the previous study (Prange and Margulies 2002).

Infant cranial bone was modeled as orthotropic elastic in plane stress with different elastic moduli parallel and perpendicular to fiber orientation Eq. [1, 2].

$$\begin{bmatrix}\sigma_1\\ \sigma_2\\ \sigma_{12}\end{bmatrix}=\begin{bmatrix}\frac{E_1}{1-\nu_{12}\nu_{21}} & \frac{\nu_{12}E_2}{1-\nu_{12}\nu_{21}} & 0\\ \frac{\nu_{21}E_1}{1-\nu_{12}\nu_{21}} & \frac{E_2}{1-\nu_{12}\nu_{21}} & 0\\ 0 & 0 & G\end{bmatrix}\begin{bmatrix}\varepsilon_1\\ \varepsilon_2\\ 2\varepsilon_{12}\end{bmatrix} \quad [1]$$

$$G=\frac{E_1}{2(1+\nu_{12})} \quad [2]$$

The average elastic modulus of infant parietal and occipital cranial bone tested perpendicular to the fiber orientation from donors age 0.5-2.5 months is reported as 453 and 300 MPa, respectively (Coats and Margulies 2006, Table A1 in Appendix) and was used for E_1 in Eq. [1]. For the orthotropic material model the modulus parallel to the fiber orientation was assumed to be four times stiffer ($E_{2\_parietal}$=1810 MPa, $E_{2\_occipital}$=1200 MPa) based on direction-specific infant cranial bone data from McPherson and Kriewall (1980a). The shear modulus, G, was assumed to be isotropic and computed using Eq. [2]. The Poisson's ratio, ν_{12}, used in Eq. [1] and [2] was assumed to be that of adult cranial bone when compressed radially (McElhaney, et al. 1970). The Poisson ratio, ν_{21}, was calculated from Eq. [3] with the assumption that in-plane stress components on perpendicular faces must be equal in magnitude (Crandall, et al. 1978).

$$\nu_{12}E_1=\nu_{21}E_2 \quad [3]$$

The material response of infant cranial suture was modeled as linear elastic. The average elastic modulus of coronal suture for 0-12 month old infants is reported as 8.1 MPa, with no significant effect of donor age (Coats and Marguiles 2006, Table A2 in Appendix) and the elastic modulus of the model was assigned as this value. The Poisson's ratio and density of pediatric cranial suture is unknown, and suture was assumed to be incompressible with a density equal to that of dura (Galford and McElhaney 1970). It is unknown whether location plays a significant role in the material properties in suture, and the modulus of coronal suture was used to represent all sutures in the finite element model.

The scalp of a 1 month old male infant ranges from 1.9-9.1 mm with a median of 3.5 mm (Young 1959), thus a thickness of 3.5 mm was used in the model to represent a 1.5 month old child. Scalp was modeled as linear elastic using properties measured in adult monkey (Galford and McElhaney 1970).

Table 1. Summary of material properties used in infant finite element model.

Material	*Properties*	*Source*
Brain	μ=559 Pa α=0.00845	Scaled from Prange and Margulies (2002)
	ρ=1.04x10^3 kg/m^3 ν=0.499	Prange (2002)
Skull	ρ=2.09x10^3 kg/m^3 ν_{12}=0.19	Kriewall (1981) McElhaney et al. (1970)
Parietal	E1=453 MPa E2=1810 MPa G=662 MPa	Coats and Margulies (2006, 0.5-2.5 month olds)
Occipital	E1=300 MPa E2=1200 MPa G=503 MPa	Coats and Margulies (2006, 0.5-2.5 month olds)
Suture	ρ=1.13x10^3 kg/m^3 ν=0.49	Galford & McElhaney (1970)
	E=8.1 MPa	Coats and Margulies (2006, < 1 year old)
Scalp	ρ=1.2x10^3 kg/m^3 ν=0.42 E=16.7 MPa	Galford & McElhaney (1970)

Boundary Conditions. Frictional contact (μ=0.20) was used to model the interaction between the rigid plate and the skull as well as that between the brain and inner surfaces of the skull (Ji and Margulies 2007; Miller, et al. 1998). The foramen magnum of the skull was left open, allowing the brain to move freely past this boundary (Ji and Margulies 2007). Suture nodes were tied to the skull along the perimeter of the suture.

Loading Conditions. For parametric and convergence analyses, a direct impact to the occiput following a 0.3m fall onto concrete was simulated. All components of the infant head model were provided with an initial velocity moving in a direction towards a fixed rigid body plate. The initial velocity was set equal to 2.44 m/s, the ideal velocity at impact from a 0.3 m fall calculated using the law of conservation of energy.

Mesh Development. All meshing and element definitions (Table 2) were made in Patran (MSC Software Corp, Santa Ana, CA) for analysis in ABAQUS/Explicit (ABAQUS, Inc, Providence, RI) and run on a Dell Precision 470 computer with 3.4 GHz, an Intel Xeon CPU and 2 GB of RAM (Dell

Inc., Roundrock, TX). Tetrahedral 10-noded elements were used for all brain tissue (CD10M). Hexagonal 8-noded solid elements were used to model scalp (C3D8R). Hexagonal 8-noded continuum shell elements (SC8R) were used to model both occipital and parietal cranial bone. These continuum shell elements have the 3D geometry of solid elements, but with the bending behavior of shell elements. Two-dimensional 4-noded membrane elements (M3D4R) with a thickness of 1.18 mm (average suture thickness measured from Coats and Margulies, 2006) were used to model the suture. The combined hourglass energy for all components of the FEM was required to be less than 10% for all simulations. A convergence study was conducted to evaluate the stability of the finite element mesh.

Table 2 Number and type of elements used in finite element model of occipital head impact in infants.

Model Component	*No. of Elements*	*Type of Element*	*ABAQUS Element Label*
Brain	11,066	Tetrahedral 10-noded solid element	C3D10M
Scalp	624	Hexagonal 8-noded solid element	C3D8R
Skull			
Parietal	16,434	Hexagonal 8-noded continuum shell element	SC8R
Occipital	2,272*		
Suture	2,485	4-noded membrane element	M3D4R

**Final number of elements determined from convergence study. Some additional elements along the base region of the skull were categorized in the occipital group, but were not subject to direct impact, so they were not included in the convergence study.*

Material Model Validation

To validate the cranial bone and suture material models and their assumptions, two finite element models were created to simulate a cranial bone three-point bone bending test and cranial suture tensile test previously reported for a 1.5 month old infant (Coats and Margulies 2006). The computational model geometry mimicked the actual specimens in the experimental tests, and properties and elements used were those values described above and presented in Tables 1 and 2 for cranial bone and suture.

Pediatric Head Model Parametric Study

A parametric study was performed to determine the relative influence of the following input parameters of the pediatric head model: brain material property stiffness, brain compressibility, suture thickness, suture width, and scalp presence. These parameters were selected because values reported in the literature vary or there exists natural anatomical variations in human infants. Baseline values for each of the parameters (Table 3) were selected from empirical measurements and published data from our lab (Coats and Margulies 2006; Prange and Margulies 2002).

Brain Material Properties. Given the deformable nature of the infant skull, the stiffness and compressibility of the pediatric brain may significantly influence the response of the pediatric skull to impact. Baseline brain material parameters used in the model were scaled from published human adult values based on the ratio between the properties in adult and newborn porcine gray matter reported in a previous study (Prange and Margulies 2002). However, there exists a wide range of reported adult brain shear moduli (Bilston, et al. 2001; McCracken, et al. 2005; Prange and Margulies 1999). Shear moduli from both ends of the spectrum (257 Pa and 2.17 kPa) were used in two of the parametric simulations (P1 and P2, respectively) to determine the effect of brain stiffness on principal stress (σ_p) in pediatric skull.

Adult brain tissue has been shown to be an incompressible material with a bulk modulus of approximately 2.1 GPa (Lippert, et al. 2004; McElhaney, et al. 1972). Unfortunately, some compressibility must be assigned for the algorithms of dynamic solid elements to work efficiently in the computational modeling program (ABAQUS/Explicit). While increasing the compressibility of the model increases the stability and computational efficiency of the model, it also decreases the bulk modulus below those reported for adult human brain. To determine the influence of the increase in brain compressibility (and decrease in bulk modulus) on σ_p of the infant skull, three commonly used values for Poisson's ratio were selected for baseline (ν=0.499) and two of the parametric simulations (P3: ν= 0.49, P4: ν= 0.4999). Using the estimated shear modulus of pediatric human brain (μ=558 MPa), the corresponding bulk moduli for ν=0.49, 0.499, and 0.4999 are 27.8 kPA, 279 kPa, and 2.79 MPa, respectively.

Skull and Suture Anatomic Variations. In order to obtain accurate skull geometry, MRI and CT images from a 5-week old infant were used. While these images can provide an accurate representation of skull thickness, it can be difficult to determine exact suture width and thickness, and anatomical variations naturally exist in infants. To determine the effect

these variations may have on σ_p of infant skull, half the suture thickness (P5; 0.49 mm), no suture (P6) and more than twice the largest suture width measured from the CT images (P7; 10 mm) were used for three of the parametric simulations. All the sutures in the skullcase were modified according to the specifications of P5, P6, and P7, but the fontanels were only modified in P5 and P6.

Scalp Inclusion. To determine the effect scalp has on principal stress in the highly deformable skullcase of the infant following an impact from a low height fall, a parametric simulation (P8) excluding scalp was performed.

Parametric Loading Conditions. To determine the relative influence of these parameters (Table 3) on the prediction of skull fracture, a 0.3m fall with an impact to the occiput onto concrete was simulated. Changing just one parameter value for each parametric simulation, the maximum σ_p of each element of the occiput over all time points in the parametric simulation was compared to that of the baseline counterpart.

Comparisons were made between the response of individual skull elements of the baseline model and those of the parametric simulations. Because elements within a mesh are influenced by their neighboring elements, no statistical analyses were appropriate, but we report differences in maximum principal stress, contact force, contact area, and impact duration for each parametric simulation as a percent of the baseline value.

Pediatric Head Model Validation

To validate the model's ability to predict fracture from impact onto hard surfaces, a computational simulation of a parietal-occipital impact onto a fixed rigid plate (Figure 2) was performed. The prediction of fracture from the simulation was compared to free-fall infant cadaver studies onto stone tile (Weber 1984).

The definition of fracture in the validation is determined by comparing the principal stress of the skull elements in the FEM to the ultimate stress of cranial bone for 0.5-2.5 month old infants as published previously (Coats and Margulies 2006, Table A1 in Appendix). To avoid spurious, isolated elements, a 3×3 elemental array containing the highest stress values was selected at each time point and for each cranial bone of the impact region (occipital, left parietal and right parietal). Fracture was said to occur if the average stress of the element array was greater than the ultimate stress of cranial bone at any time during the simulation.

Table 3. List of parameters investigated for parametric study. Bold values were selected based on results of parametric study to be used in the model validation.

Parameter	*Baseline*	*Parametric Simulation Value*
Brain Stiffness	**559 Pa**	
P1 – Adult (Prange 2002)		257 Pa
P2 – Adult (Bilston 2001)		2.19 kPa
Brain Compressibility	0.499 (K=279 kPa)	
P3		0.49 (K=2.78 kPa)
P4		**0.4999 (K=2.79 MPa)**
Suture Thickness	**1.18 mm** (ave. skull)	
P5 – ½ skull thickness		0.59 mm
Suture Width	**2-3mm** (CT)	
P6 – no suture		0 mm
P7 – wide suture		10 mm
Scalp Inclusion	**Yes**	
P8 – no scalp		No

Figure 2. Parietal-occipital impact simulating published infant cadavers from 0.82 cm onto stone.

The normal distribution of ultimate stress from the 0.5-2.5 month old data was used to determine a probability of fracture from our model. Element arrays with an average stress value above the mean ultimate stress of occipital or parietal bone (9.4 or 27 MPa, respectively) were defined as having a 50% probability of fracture. An average stress above (or below) 1 standard deviation from the mean was defined as having an 84.1% (or 15.9 %) probability of fracture, above (or below) 2 standard deviations from

the mean was defined as having a 97.7% (or 2.3%) probability of fracture and above (or below) 3 standard deviations from the mean was defined as having a 99.8% (or 0.2%) probability of fracture. The probability of fracture determined from our model was compared to that reported by Weber.

RESULTS

Mesh Convergence Study

The convergence study to evaluate the stability of the finite element mesh resulted in an impact region with 1,871 elements with an average element edge length of 1.3 mm. This density was selected as the optimal mesh because of its minimal residual error (Figure 3) and its significantly shorter computational time when compared to the densest mesh.

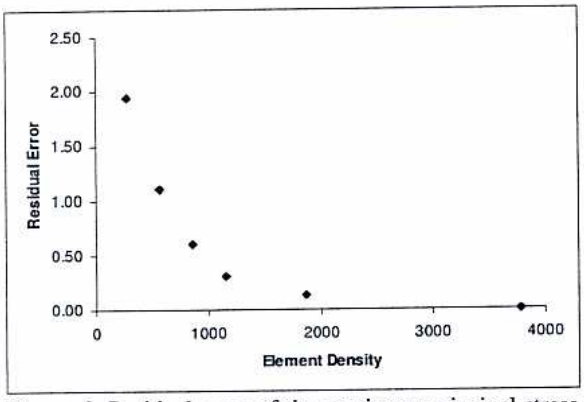

Figure 3. Residual error of the maximum principal stress calculated for each mesh density compared to the densest mesh for the convergence study. The mesh with 1,871 elements in the impact region was selected because of its outcome variable stability and allowable computational time (~80 hrs).

Material Model Validation

The ultimate stress of cranial bone calculated from the experimental three-point bending test (σ_{ult_test}) was compared to the maximum principal stress predicted from the cranial bone finite element model (σ_{princ_model}) at 26 msec (time at which fracture occurred in the bending test). The results of the finite element model found good correlation with the results from the bending test (σ_{princ_model} = 19.3 MPa, σ_{ult_test}=19.7 MPa), indicating that material model formulations (Eq. [1]-[3]) and its assumptions were acceptable. Principal stress was the most accurate determinate of ultimate stress and was selected as the outcome variable for the prediction of fracture in the model validation.

The close correlation of the ultimate logarithmic strain of an actual cranial suture tension test ($L\varepsilon_{ult\_test}$) to the maximum logarithmic strain in the finite element model ($L\varepsilon_{princ\_model}$) at 1.5 msec (time to reach failure in tension test) indicated that this material model was a good representation of empirical data ($L\varepsilon_{princ\_model}$ = 0.8 mm/mm, $L\varepsilon_{ult\_test}$=0.75 mm/mm).

Pediatric Head Model Parametric Study

Brain Material Properties. The maximum principal stress (σ_{p_max}), peak contact force, contact area, and impact duration between simulations using the baseline brain shear modulus (pediatric scaled from adult) and those using adult brain modulus (P1) from Prange (2002) were found to differ by less than 1% (Table 4, Figure 4A). However, increasing the brain stiffness by a factor of 4 in pediatric simulations (P2) to values similar to the adult bovine brain shear moduli reported by Bilston (2001) for small strains increased the σ_{p_max} experienced by the skull by 38% of baseline and increased peak force by 27%. From this data, it appears that decreasing the brain stiffness 50% does not influence the skull stress response to impact, but a much stiffer brain (an increase of 1600 Pa from pediatric baseline) will increase the stresses of the deformable infant skull.

Parametric simulations varying brain compressibility (and thus significantly altering the bulk modulus) found a 52% difference in σ_{p_max} when altering the compressibility from 0.49 (P3) to 0.4999 (P4), indicating that the skull is highly influenced by the bulk modulus of the brain. An order of magnitude softer bulk modulus than baseline (K=27.8 kPa) decreased σ_{p_max} by 29.7% and peak contact force by 23.4%, while a magnitude larger bulk modulus than baseline (2.79 MPa) increased the σ_{p_max} by 47.7% and peak contact force by 42.3%. Interestingly, there was a significant alteration to the force-time response when adjusting the value of the compressibility (Figure 4B).

Because the brain compressibility greatly influences the principal stress of the skull (and thus the prediction of fracture), the Poisson's ratio associated with a bulk modulus closest to that reported for adult brain (ν=0.4999) was used in the head model validation simulations. If the model validation using

Table 4. Results from parametric simulations of a 0.3m fall onto concrete. Bold values indicate a change of 15% or more from baseline.

	Peak Principal Stress (MPa)	*Peak Force (N)*	*Max Contact Area (mm^2)*	*Contact Duration (ms)*
Baseline	29.5	391	384	10.8
P1 – Brain stiffness $\mu = 257$ Pa	29.5	395	384	10.8
P2 – Brain stiffness $\mu = 2.19$ kPa	**40.8**	**498**	**560**	9.25
P3 – Brain incomp. $\nu = 0.49$	**20.8**	**299**	368	**4.50**
P4 – Brain incomp. $\nu = 0.4999$	**43.7**	**555**	**593**	**9.20**
P5 – Suture thickness $t = 0.59$	30.0	376	384	11.0
P6 – No suture	29.5	417	416	10.8
P7 – Large suture W = 10 mm	**16.8**	**284**	352	**>15.0**
P8 – No Scalp	27.5	383	**69.2**	11.0

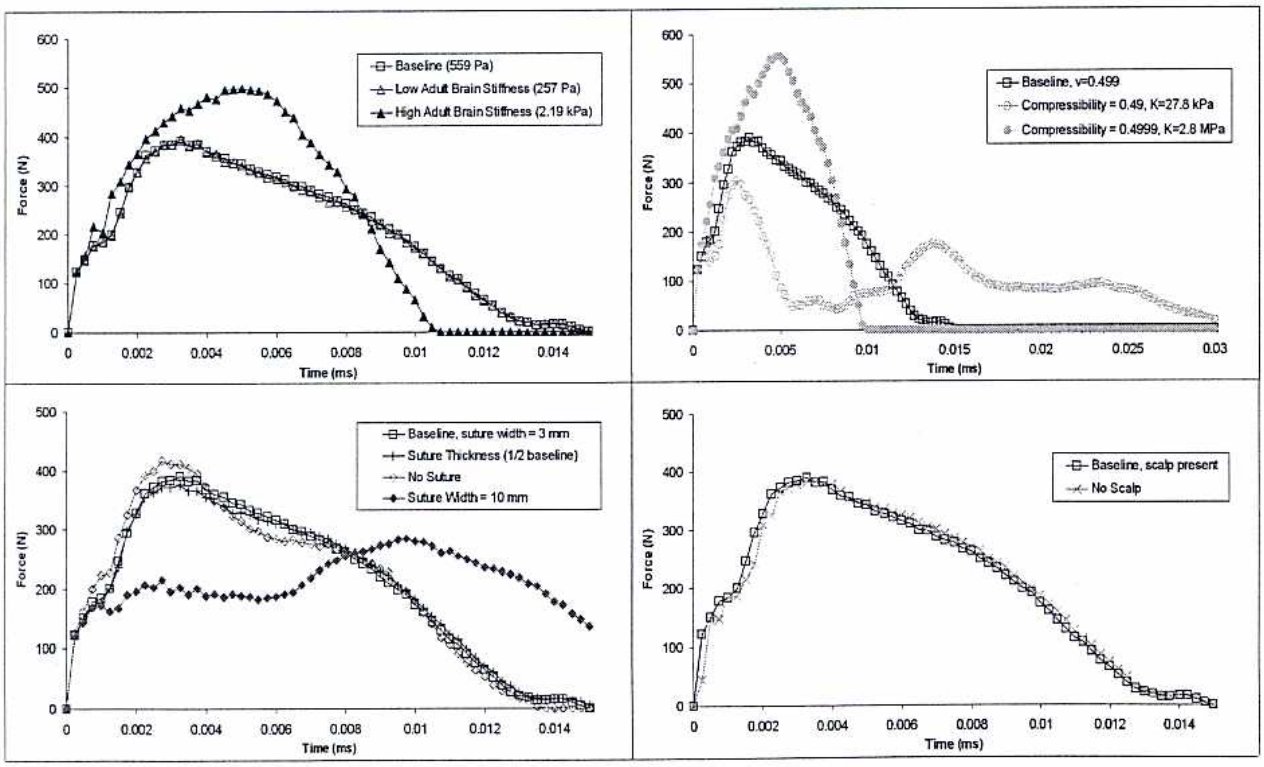

Figure 4. Force-time contact curves for the different parametric simulations: (A) brain stiffness, (B) compressibility, (C) suture anatomy, and (D) scalp inclusion. All simulations measured the skull response for 15 ms, except for the parametric simulation with a compressibility of 0.49 which required a longer duration of 30 ms to complete the impact.

a bulk modulus of 2.79 MPa resulted in σ_p values above the ultimate stress of cranial bone, predicting skull fracture as Weber reported, then we will conclude that a bulk modulus of 2.79 MPa is sufficiently accurate to represent the intracranial contents.

Skull and Suture Anatomical Variations. The σ_{p_max} of the elements of the occiput in the baseline simulation were 1.4% lower than that of the corresponding elements in the parametric simulation (P5) and peak contact force only decreased by 3.4% (Figure 4C). From these data, it appears that decreasing the suture thickness by ½ have only modest influence on σ_{p_max}, and thus the prediction of skull fracture. Given the minimal difference in the regional σ_{p_max}, a constant thickness of 1.18 mm (baseline) was used in the validation of the model.

There was less than 1% difference between the σ_{p_max} of the individual elements of normal suture (baseline) and those in the corresponding elements in the parametric simulation with no suture (P6), but σ_{p_max} decreased from baseline by 43.2% in the parametric simulation with a larger suture width (P7; 10 mm). A wider suture also decreased the peak contact force by 27.4% and increased the impact duration by at least 38.9% (Figure 4). In summary, the width of the suture plays an important role in the mechanical response of the infant head to impact. For model validation, the widths measured (regionally varying 2-3 mm) from the CT images (baseline) were used since the CT images were from a normal 1.5 month old infant and lie within the published range of 1-2 month old children (regionally varying 0.35-3.2 mm; Soboleski et al. 1997).

Scalp Inclusion. Contact force, impact duration, and maximum principal stress of the skull differed less than 2% between the parametric simulation excluding scalp (P8, Figure 4D) and baseline. However, the simulation with no scalp had a significantly decreased contact area (-82.0%) when compared to the baseline with scalp. While this decrease in contact area did not affect the peak force or duration of the impact for the one foot fall, a fall from higher heights may have more significant effects. For this reason, scalp was included in the pediatric head model validation.

Pediatric Head Model Validation

Based on results from the parametric study, only the value used for the compressibility of the brain was altered from the baseline simulation and used in the model validation (Table 3, bold). The σ_{p_max} (as determined by the average principal stress of the 3×3 element array) across all time points for the simulations of parietal-occipital impact from an 82 cm fall onto concrete occurred in the parietal bone and reached levels of 70.0 MPa (Figure 5). The σ_{p_max} for a drop onto concrete is greater than 3 standard deviations above the mean value we reported for the ultimate stress of parietal bone, indicating a 99.8% probability of fracture from an 82 cm fall onto concrete. The skull geometry in the model contained a natural irregular midline convexity on the occipital bone in the region of the parietal-occipital impact. Thus, after the initial impact this curvature forced the contact region of the skull with the plate to rotate towards the left parietal bone. For this reason, the probability of fracture on that side is twice as high as the probability of fracture on the right parietal bone.

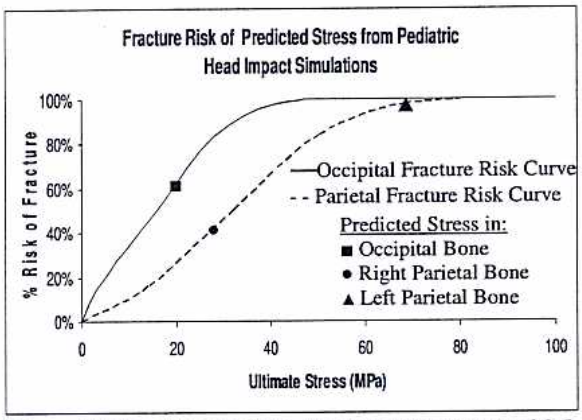

Figure 5. The ultimate stress data for cranial bone of 0.5-2.5 month old infants published by Coats and Margulies (2006) and given in Table A1 were analyzed as discussed in the Methods section to create the occipital and parietal fracture risk curves shown on the graph. Maximum principal stress values in the occipital (■), right parietal (●), and left parietal (▲) bones show that simulated cadaver drops from a height of 82cm onto stone tile result in a 99.8% probability of fracture on the left parietal bone of the skull.

DISCUSSION

While computational models are fairly commonplace for adult head injury research, very few pediatric computational models exist due to the small number of pediatric material property data. Previous models have been forced to rely on adult or animal material properties (Klinich, et al. 2002), but a recent study reports that the material properties of human infant cranial bone and suture are one order or more than 3 orders of magnitude less stiff than porcine pediatric cranial bone and suture, respectively (Coats and Margulies 2006). These large differences would likely influence the cranial response in prior finite element models of the pediatric skullcase to impact. Thus, we developed a 1.5 month-old infant finite

element model that is the first to incorporate this recently published material property data of infant cranial bone and suture tested at high strain rates (9-100 s^{-1}). Due to the paucity in human pediatric brain material property data and natural anatomical variations in the infant skullcase, a parametric study was performed prior to validation to determine the effects of brain stiffness, brain compressibility, suture width and suture thickness on the principal stress response of the pediatric skullcase to impact.

Brain Material Properties

Brain Stiffness. Pediatric porcine tissue has been shown to be more than twice as stiff as adult porcine tissue measured at large strain deformations (Prange and Margulies 2002). Thus, the pediatric material constants used in the baseline model were actually 2 times stiffer than the adult human values measured by Prange (2002). No significant effect on σ_p was found between the pediatric baseline simulation and the parametric simulation using the adult value measured by Prange. However, recent studies have measured adult brain shear modulus to be much higher than those reported by Prange. McCracken et al. (2005) used MR elastography to predict adult human brain shear modulus and reported 7.5±1.6 kPa as the average shear modulus of adult cortical gray tissue. This shear modulus is nearly 4 times greater than the pediatric baseline value and is similar to that of adult bovine brain as reported by Bilston et al. (2001). In our simulations, the stiffer shear modulus of adult bovine brain was found to increase the σ_{p_max} of the skull by 38% compared to the baseline and it is anticipated that a parametric study using the values reported by McCracken et al. would also increase the σ_{p_max} of the skull. The stiffest human adult brain shear modulus reported (Shuck and Advani 1972) is 3 orders of magnitude stiffer (μ=528 kPa) than the pediatric baseline value. This shear modulus was measured at very small strains and high frequencies. In these conditions, this stiff brain tissue would be expected to even further increase the σ_{p_max} experienced by the pediatric skull during impact.

From these parametric simulations, decreasing the brain stiffness does not influence the skull stress response to impact, but a much stiffer brain will significantly increase the stresses of the deformable infant skull. Thus, caution should be exercised when selecting brain tissue properties.

Brain Compressibility. The σ_p response of the infant skull was found to be extremely sensitive to the Poisson's ratio used to represent brain compressibility in the computational model. Smaller Poisson's ratios improve algorithm efficiency, but they also make the bulk response of the model much softer than that of the actual material. This softer bulk modulus increases brain deformation and consequently provides less resistance to the skull during impact.

The algorithms of the computational model pose a natural limitation to the model. To determine a value for our model that provided a realistic pediatric skull response while maximizing computational efficiency, the shape of the force-time response and the peak impact force value were compared to cadaver drops in the literature and surrogate impact drops from our lab. Prange et al. (2004) dropped 3 neonatal cadaver heads (1, 3, & 11 days old) from < 0.3 m onto a metal anvil and measured the impact force-time trace using a 3-axis piezoelectric load cell. The measured trace for all measured impacts had a distinct parabolic shaped curve (Figure 6A). Only the parametric simulation using a Poisson's ratio value of 0.4999 mimicked this measured force-time response shape. This Poisson's ratio had the stiffest bulk modulus (K=2.79 MPa) used in our study. The lower Poisson's ratios, v=0.49 and v=0.499, resulted in bulk moduli of 27.8 and 279 kPa, respectively. The much lower bulk modulus of 27.8 kPa created a softer, more deformable brain that allowed the occipital skull to deform until it made contact with the left and right parietal bones. This bone-to-bone contact shortened the time duration of the impact (Figure 6B), decreasing the impulse of the impact by about 3 times that in the simulations using the larger bulk moduli.

The peak impact force measured by Prange is closer to the peak impact force from our simulations using 0.49 and 0.499 and the impulse for the cadaver force-time response is 2.38 N*s compared to 3.54 N*s from our simulation using 0.4999. These differences are likely due to the anatomical and age differences between the pediatric cadaver head and the head simulation in this study. The 11-day old infant cadaver was born several weeks premature, had a lower head mass than the head in our simulation (0.65 vs 0.87 kg), and had unusually large sutures (23 mm). The elastic modulus of infant cranial bone significantly increases with age (Coats and Margulies 2006) and our parametric study found that a suture width of 10 mm decreased the peak impact force by 27.4% when compared to an infant with suture widths varying from 2-3 mm. Thus, a lower impact force and longer impact duration would be expected when compared to simulations of a 1.5 month old infant. The lower head mass would contribute to the lower impulse of the impact.

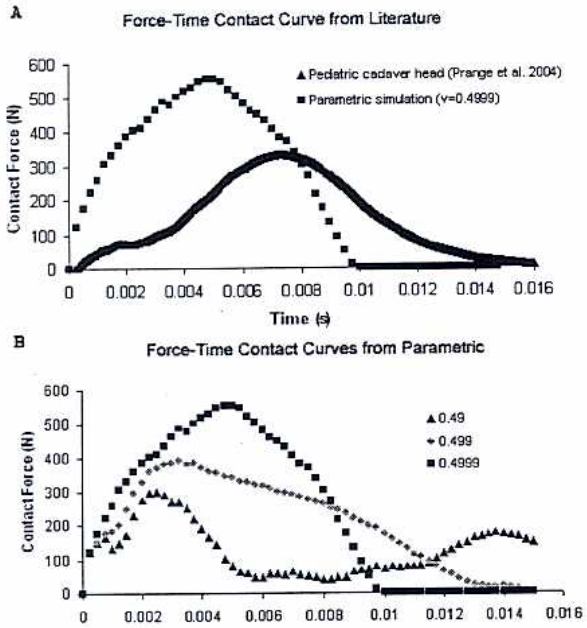

Figure 6. (A) A value of 0.4999 most closely represents the *parabolic* shape of the force-time impact curve reported in the literature for an infant cadaver head impacting a steel surface from a one foot height (Prange, et al. 2004). (B) The value used to represent incompressibility in the finite element model significantly affected the shape of the force-time response curve. *Note:The infant cadaver dropped in (A) was premature with a lower head mass and unusually large sutures, resulting in a lower impact force and longer impact duration than our simulations in B.*

The bulk modulus of adult human brain has been measured as 2.1 GPa (Lippert, et al. 2004; McElhaney, et al. 1972). No bulk modulus studies of pediatric brain exist in the literature and developmental changes (e.g., axon myelination) may distinguish the bulk modulus of the pediatric brain from the adult brain. Additionally, the model in this study does not incorporate separate structures for ventricles in the brain, and the compression of these spaces in the human brain likely increases the composite compression of the intracranial contents. The model validation found that the bulk modulus of 2.79 MPa was sufficient to simulate the pediatric skull response to impact onto a hard surface. Dynamic computational model algorithms pose a numerical limitation to FEM, and only model validation is able to determine whether a softer bulk modulus in the pediatric brain will provide sufficiently accurate results in a specific scenario simulated. Further examination of bulk modulus will need to be performed for validating this pediatric head model onto softer surfaces. Other computational modelers should be careful when selecting the compressibility of brain for their simulations and use validation to verify their assumptions.

Skull and Suture Anatomical Variations

Normal anatomical variations exist within the infant skull and suture, and it is important to determine the effect these variations may have on the response of the model. The value selected for the baseline suture thickness in the parametric study (1.18 mm) was the average thickness measured from 0.5-2.5 month old infant cranial suture material property testing. Paired comparisons of elements from simulations with suture thickness of 0.59 mm did not alter the overall σ_{p_max} of the impact region significantly from baseline simulations. Thus, suture thickness was considered not to have a significant effect on the prediction of fracture from impact to the infant skullcase.

The suture width selected for the baseline infant model was measured from the CT images and varied between 2-3 mm, depending on the suture location. An average suture width for infants 1-2 months has been measured by sonography in the literature as ranging from 0.35-3.2 mm, depending on suture location (Soboleski, et al. 1997). Children within this same age group have also been documented to have unusually large suture widths (Loyd, et al. 2004) The parametric study found that eliminating the 2-3 mm suture did not affect the σ_{p_max} of the impact region, but that widening the suture width to 10 mm significantly decreased the σ_{p_max} of the entire impact region by more than 40%. Therefore, this model is only applicable for infants whose sutures remain within the normal range of suture widths (0.35-3.2 mm) and would over predict the presence of fracture in infants with unusually large suture widths.

Scalp Inclusion. The exclusion of scalp in our pediatric head model had minimal effect on the contact force, impact duration, and σ_{p_max} in the skull. This finding is consistent with the results of the Klinich et al (2006) finite element model parametric study that reports decreasing the stiffness of the scalp by an order of magnitude (17 MPa to 1.7 MPa) in a model of head impact to a 6-month old infant changes stress in the occipital and parietal bones by less than 1% and has no effect on peak head acceleration. The parametric simulations in this paper and the Klinich et al. paper agree that the stress in the deformable pediatric skull due to impact is affected more by the material properties of the pediatric skullcase and the brain than the overlying scalp.

Pediatric Head Model Validation

To validate the computational model and its assumptions, a study of infant cadaver drops onto a hard surface was simulated. Weber (1984; 1985) dropped 40 infant cadavers (1.1-9.0 months) onto the parietal-occipital region of the skull from a supine position 82 cm above stone tile, carpet, foam-padded linoleum, a folded camel hair blank, and a 2 cm thick foam pad. All 5 (100%) of the cadavers dropped onto the stone tile had skull fracture (Table A3, Appendix).

Sketches of fracture locations indicate that the majority of the fractures from drops onto stone tile and foam pad initiated at the parietal-lamboidal suture boundary and propagated toward the center of the parietal bone. Our simulations of a fall onto a rigid surface predict a high probability of fracture with the largest stress concentrations at the parietal-lamboidal suture boundary. Both the probability and highest stress location correspond well to the probabilities and fracture location detailed by Weber.

The maximum principal stress in the left parietal bone was approximately twice as large as that of the right parietal bone in the simulation. The natural geometry of the infant skull has a bony curvature on the upper region of the occipital bone. An impact to the occipital-parietal region of the skull hits this curvature and causes the impact to rotate to either the right or left side of the apex of the curvature. In our simulation, the impact contact region rotated to the left side of the skull, concentrating the impact to the occipital and left parietal bone. A shift in the impact region would likely cause it to rotate to the right side of the curvature and impact predominantly the occipital bone and the right parietal bone. Given this curvature and the location of the parietal-occipital impact simulated, it would be rare that the impact would be equally distributed among the right and left parietal bones. Sketches of fracture locations from Weber studies agree with our findings and rarely show fracture in both right and left parietal bones (Table A3, Appendix), but rather have fractures that are associated with either the left or right parietal bone. Only 1 out of the 21 fractures that Weber reports had both right and left parietal fracture. However, 2 out of the 21 had only occipital fracture and it is possible that this may be due to the equal distribution of impact force to the left and right parietal bones.

The complex nature of fracture poses a significant challenge to predicting the cranial stress and strain response after the initiation of fracture. Therefore, this model makes no predictions as to the severity or type of fracture that can occur. More detailed fracture and crack propagation algorithms would need to be incorporated into the model and validated before this type of prediction could be made. Additionally, the brain was modeled as homogenous with no distinction between white and gray matter and no inclusion of the ventricles, falx cerebri or tentorium. Thus, despite the highly deformable nature of the infant skull, one should not infer the brain deformation and associated brain injury using our model.

CONCLUSION

Using recently published material property data from 0.5-2.5 month old infant cranial bone and suture, a geometrically accurate computational finite element model was developed to predict skull fracture resulting from impact. A parametric study found that decreasing brain shear modulus in half does not significantly affect the maximum principal stress resulting from impact to the pediatric skullcase, but much stiffer brain material properties (> 1 order of magnitude) will dramatically increase the principal stress of the cranial bone. Additionally, the Poisson's ratio selected to represent the compressibility of the human brain significantly alters bulk modulus and dramatically varied the principal stress in the skull by 30-77%, underscoring the importance of determining an appropriate compressibility in computational models. Small variations in suture geometry did not alter maximum principal stress of the infant skull, but unusually large sutures (>10mm) significantly decreased the predicted occurrence of fracture from impact, demonstrating that unusual anatomic variations can have a profound effect on the injury risk.

Based on comparisons to cadaver studies, this model was a good predictor of skull fracture due to impact onto a hard surface. Validation onto softer surfaces needs to be completed before predictions for these conditions may be made. In conclusion, this new computational model incorporates recent material property and failure data of human pediatric cranial bone and suture, and can provide valuable insight into the mechanics of head impact in infants, which may be useful in the development of infant car seats and other accident prevention equipment.

ACKNOWLEDGMENTS

The authors would like to thank the following funding sources for their support of this work: NIH R01 NS39679 and CDC NCIPC R49/CE000411-01

REFERENCES

Al-Bsharat, A., Hardy, W., Yang, K., Khalil, T., Tashman, S. and King, A. (1999) Brain/skull relative displacement mognitude due to blunt head impact: new experimental data and model. 43rd Stapp Car Crash Conference SAE San Diego, CA

Bilston, L., Liu, Z. and Phan-Thien, N. (2001) Large strain behaviour of brain tissue in shear: some experimental data and differential constitutive model. Biorheology 38(4): 335-345

Bylski, D.I., Kriewall, T.J., Akkas, N. and Melvin, J.W. (1986) Mechanical behavior of fetal dura mater under large deformation biaxial tension. Journal of Biomechanics 19(1): 19-26

Coats, B. and Margulies, S.S. (2006) Material properties of human infant skull and suture at high rates. Journal of Neurotrauma 23(8): 1222-1232

Crandall, S., Dahl, N. and Lardner, T. (1978) An Introduction to the Mechanics of Solids. McGraw-Hill Singapore

Crelin, E.S. (1969) Anatomy of the newborn: an atlas. Lea & Febiger Philadelphia

DiMasi, F., Eppinger, R. and Bandak, F. (1995) Computational analysis of head impact response under car crash loadings. 39th Stapp Car Crash Conference 425-438 San Diego, California

Galford, J. and McElhaney, J. (1970) A viscoelastic study of scalp, brain, and dura. Journal of Biomechanics 3(2): 211-221

Ji, S. and Margulies, S.S. (2007) In vivo pons motion within the skull. Journal of Biomechanics 40(1): 92-99

Kleiven, S. and von Holst, H. (2002) Consequences of head size following trauma to the human head. Journal of Biomechanics 35(153-160

Klinich, K., Hulbert, G. and Schneider, L. (2002) Estimating infant head injury criteria and impact response using crash reconstruction and finite element modeling. Stapp Car Crash Journal 46(November): 165-194

Krabbel, G. and Appel, H. (1995) Development of a finite element model of the human skull. Journal of Neurotrauma 12(4): 735-742

Lapeer, R.J. and Prager, R.W. (2001) Fetal head moulding: finite element analysis of a fetal skull subjected to uterine pressures during the first stage of labour. Journal of Biomechanics 34(9): 1125-1133

Lippert, S.A., Rang, E.M. and Grimm, M.J. (2004) The high frequency properties of brain tissue. Biorheology 41(681-691

Loyd, A., Luck, J., Buraglia, N., Myers, B., Frush, D. and Nightingale, R. (2004) Thresholding techniques for developing geometrically accurate pediatric skull and cervical spine models. Injury Biomechanics Research: Proceedings of the 32nd International Workshop 61-70 Nashville, TN

McCracken, P., Manduca, A., Felmlee, J. and Ehman, R. (2005) Mechanical transient-based magnetic resonance elastography. Magnetic Resonance in Medicine 53(3): 628-639

McElhaney, J.H., Fogle, J.L., Melvin, J.W., Haynes, R.R., Roberts, V.L. and Alem, N.M. (1970) Mechanical Properties of Cranial Bone. J Biomech 3(495-511

McElhaney, J.H., Melvin, J.W. and Roberts, V.L. (1972) Dynamic characteristics of the tissues of the head. Proceedings of the 1972 Biomedical Engineering Conference Glasgow, Scotland

McPherson, G. and Kriewall, T. (1980a) The elastic modulus of fetal cranial Bone: a first step toward understanding of the biomechanics of fetal head molding. Journal of Biomechanics 13(9-16

Miller, R., Margulies, S., Leoni, M., Nonaka, M., Chen, X., Smith, D. and Meaney, D. (1998) Finite element modeling approaches for predicting injury in an experimental model of severe diffuse axonal injury. Proceedings of 42nd Stapp Car Crash Conference 155-167 SAE Tempe, AZ

Prange, M., Luck, J., Dibb, A., Van Ee, C., Nightingale, R. and Myers, B. (2004) Mechanical properties and anthropometry of

the human infant head. Stapp Car Crash Journal 48

Prange, M. and Margulies, S. (1999) Anisotropy and inhomegeneity of the mechanical properties of brain tissue at large deformation. Prevention Through Biomechanics Novi, MI

Prange, M. and Margulies, S. (2002) Regional, directional, and age-dependent properties of brain undergoing large deformation. Journal of Biomechanical Engineering 124(244-252)

Ruan, J.S., Khalil, T. and King, A.I. (1994) Dynamic response of the human head to impact by three-dimensional finite element analysis. Journal of Biomechanical Engineering 116(1): 44-50

Shuck, L. and Advani, S. (1972) Rheological response of human brain tissue in shear. Journal of Basic Engineering 905-911

Soboleski, D., McCloskey, D., Mussari, B., Sauerbrei, E., Clarke, M. and Fletcher, A. (1997) Sonography of normal cranial suture. AJR Am J Roentgenol 168(3): 819-821

Weber, W. (1984) [Experimental studies of skull fractures in infants]. Z Rechtsmed 92(2): 87-94

Willinger, R., Kang, H.S. and Diaw, B. (1999) Three-dimensional human head finite-element model validation against two experimental impacts. Ann Biomed Eng 27(3): 403-410.

Young, R. (1959) Age changes in thickness of scalp in white males. Human Biology 31(1): 74-79

Zhang, L., Hardy, W., Omori, K., Yang, K. and King, A. (2001) Recent advances in brain injury research: a new model and new experimental data. Bioengineering Conference 831-832 The American Society of Mechanical Engineers Snowbird, UT

APPENDIX A

Table A1. Human infant cranial bone material property data from Coats and Margulies (2006) used define material properties in the model and fracture.

Cranium	Donor Age	Region	Bending Modulus (MPa)†	Ultimate Stress (MPa)†	Ultimate Strain (mm/mm)†
1	19 days old	Parietal	336.8	37.8	0.1490
2	21 days old	Occipital	550.7	5.8	0.0125
		Occipital	516.2	4.6	0.0068
		Parietal	182.7	8.4	0.0450
3	1 month old	Occipital	449.2	18.5	0.0465
		Parietal	815.5	53.7	0.0753
4	1.5 month old	Occipital	28.6	8.7	0.0068
		Occipital	57.7	13.5	0.0039
5	1.5 month old	Parietal	372.4	19.7	0.0700
		Parietal	518.2	29.6	0.0533
		Parietal	581.3	25.6	0.0639
6	1 mo, 23 day old	Occipital	421.4	15.1	0.0314
7	2 month old	Parietal	297.4	14.2	0.0515
		Parietal	522.4	27.1	0.0765
8	2 mo, 9 day old	Occipital	186.4	3.08	0.0259
		Occipital	186.1	5.7	0.0268
9	3 month old	Occipital	1317.6	43.4	0.0254
		Occipital	463.5	26.1	0.0456
		Parietal	1155.2	69.7	0.0807

†Load and displacement instrumentation accuracy is 0.02% and 1.0x10-4, respectively.

Table A2. Human infant coronal suture material property data from Coats and Margulies (2006) used as material properties in model.

Cranium	Donor Age	Elastic Modulus (MPa)†	Ultimate Stress (MPa)†	Ultimate Strain (mm/mm)†
1	21 wks gest.	N/A*	3.5	N/A
2	28 wks gest.	14.2	6.7	0.6943
		13.2	6.3	4.7029
4	32 wks gest.	4.3	4.5	2.8320
5	34 wks gest.	6.9	5.7	1.2776
6	35 wks gest.	8.1	4.2	1.1234
9	2 day old	3.8	3.7	1.2776
11	2 wks old	6.4	2.2	1.0930
		3.8	3.1	1.2014
16	1 mo, 23 day old	N/A	4.6	N/A
		N/A	7.2	N/A
18	2 mo, 9 day old	N/A	6.8	N/A
21	11 month old	4.2	4.1	1.2511
22	12 month old	16.2	3.5	0.3324

*Values not reported (indicated by N/A) were due to problems with displacement measurements. †Load and displacement instrumentation accuracy is 0.02% and 1.0x10-4, respectively.

Table A3. Summary of results from Weber (1984,1985) cadaver drops. All drops were from 82 cm. Dashed lines indicate no fracture found.

Surface	Age (mo)	Gender	Fracture Location
Stone Tile	2.3	M	L.Par.
	4	M	Occ
	4	F	L.Par, L.Fron, Occ.
	3	F	R.Par
	3.1	F	L.Par , Occ
Carpet	3.3	M	L.Par
	3	M	L.Par
	2.3	F	L.Par, R.Par
	3.2	M	L.Par
	2.3	F	R.Par,Occ
Padded Linoleum	8.1	M	R. Par
	1.2	M	L. Par
	8.2	F	Occ
	3	M	R. Par
	Newborn	M	L. Par
2 cm Foam Mat	9	F	--
	1.2	M	--
	2.3	F	--
	2	F	Location unknown
	3	M	L. Par
	1.1	M	--
	4	M	--
	3.1	M	--
	6	M	--
	2.2	F	--
Folded Camelhair Blanket	Newborn	M	--
	2.1	F	--
	3.4	M	--
	2.2	M	--
	4.3	M	--
	3.4	M	L. Par
	9.1	F	--
	4.3	F	--
	3	M	--
	2.3	M	L. Par
	2.4	M	L. Par
	5.3	F	--
	3	M	L. Par
	7	M	--
	1.4	F	--
	3	F	--
	1.2	M	--
	6.2	F	--
	2.2	M	--
	3	F	--
	3.2	F	--
	6.3	M	--
	5	M	--
	3	F	--
	2.3	F	--